

MCSCF/MP2 Study of the Cheletropic Addition of Singlet and Triplet CF_2 and $\text{C}(\text{OH})_2$ to the Ethene Double Bond

Fernando Bernardi,^{*,†} Andrea Bottoni,[†] Carlo Canepa,[‡] Massimo Olivucci,[†] Michael A. Robb,[§] and Glauco Tonachini^{*,‡}

Dipartimento di Chimica "G. Ciamician", Università di Bologna, Via Selmi 2, 40126 Bologna, Italy, Dipartimento di Chimica Generale e Organica Applicata, Università di Torino, Corso Massimo D'Azeglio 48, 10125 Torino, Italy, and Department of Chemistry, King's College, London, Strand, London WC2R 2LS, U.K.

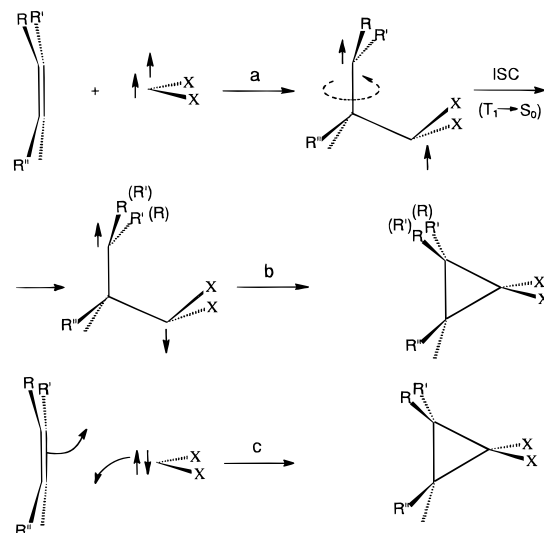
Received May 9, 1996 (Revised Manuscript Received December 3, 1996[®])

CAS-MCSCF calculations describe the addition of singlet CF_2 and $\text{C}(\text{OH})_2$ to the ethene double bond as a two-step reaction. The energy barriers that separate, in the first rate-determining step, loosely bound π -complexes from stable $\text{CH}_2\text{CH}_2\text{CX}_2$ diradical intermediates show the expected ordering, smaller for CF_2 than for $\text{C}(\text{OH})_2$. Back-dissociation of the diradicals into reactants requires the overcoming of non-negligible energy barriers. In both diradicals, the CAS-MCSCF activation energy for ring closure is smaller than that required for rotation of their terminal methylenic groups, which models, in these simple systems, an isomerization process. However, when the activation free energies are computed, in the case of the difluoro diradical the isomerization process appears to be less disfavored (and possibly competitive to some extent at higher temperatures); in contrast, in the case of the dioxy diradical, isomerization is never competitive with ring closure. The small energy barriers for ring closure of the diradicals disappear altogether when multireference MP2 energy calculations are carried out on the CAS-MCSCF critical points, casting doubts on the very existence of these intermediates. However, in contrast with the ethene reaction, the addition of singlet CF_2 to isobutene involves the formation of a diradical intermediate whose barrier for ring closure persists also at the MP2 level. These results suggest that cyclopropanation is likely to be a two-step process (with formation of a diradical intermediate) only with bulky substituted alkenes, while the attack to an unsubstituted double bond could be an asynchronous but concerted process. The analogous triplet reactions go through transition and stable structures of lower symmetry than the singlet and see the intervention of diradical intermediates. Their formation is easier than that in the singlet case and their stability with respect to back-dissociation higher. Also the isomerization processes (taking place again through rotation of the terminal methylenic group) are easier than those examined on the singlet surfaces.

Introduction

Carbenes are known to react with alkenes by adding to the carbon–carbon bond double in a cyclopropanation reaction. They can react either in a triplet or in a singlet state. Triplet carbenes are known to react in a non-stereospecific way,^{1a} and the addition mechanism is thought to involve diradical intermediates (Scheme 1, path a) whose lifetime is assumed to be sufficiently long as to allow isomerization to take place through rotation of the terminal group CRR' . This step is then followed by a decay process from the triplet state T_1 to the ground state S_0 ^{1b} through an intersystem crossing (ISC) and by ring closure to two different possible isomers. In contrast, singlet carbenes most often add stereospecifically, and the process is generally believed to occur in a single kinetic step (i.e., a concerted addition, as shown in Scheme 1, path c).^{1c}

Scheme 1



[†] Università di Bologna.

[‡] Università di Torino.

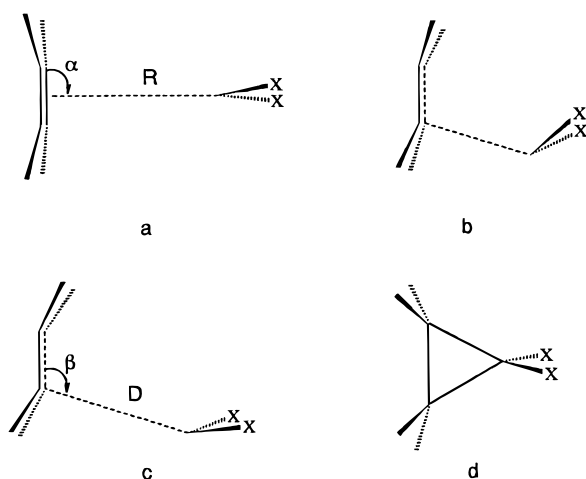
[§] King's College.

[®] Abstract published in *Advance ACS Abstracts*, February 15, 1997.

(1) (a) Skell, P. S.; Garner, A. Y. *J. Am. Chem. Soc.* **1956**, *78*, 3409–3411 and 5430–5433. Woodworth, R. C.; Skell, P. S. *J. Am. Chem. Soc.* **1956**, *78*, 4496–4497. Skell, P. S.; Klebe, J. *J. Am. Chem. Soc.* **1960**, *82*, 247–248. Jones, M.; Tortorelli, V. I.; Gaspar, P. P.; Lambert, J. B. *Tetrahedron Lett.* **1978**, *19*, 4257–4260. (b) Turro, N. J.; Ramamurthy, V.; Cherry, W.; Farneth, W. *Chem. Rev.* **1978**, *78*, 125–145. Lower, S. K.; El-Sayed, M. A. *Chem. Rev.* **1966**, *66*, 199–241. Wagner, P. J.; Hammond, G. S. *Adv. Photochem.* **1968**, *5*, 21–156. (c) Woodworth, R. C.; Skell, P. S. *J. Am. Chem. Soc.* **1959**, *81*, 3383–3386. Jones, M.; Ando, W.; Hendrick, M. E.; Kulczycki, A., Jr.; Howley, P. M.; Hummel, K. F.; Malament, D. S. *J. Am. Chem. Soc.* **1972**, *94*, 7469–7479.

The theoretical study of the addition reactions of carbenes to double bonds provides examples of systems allowed to evolve only through a non-least-motion pathway, of symmetry lower than that achieved in the products. For symmetrically disubstituted carbenes, and for methylene itself, a C_{2v} approach (Chart 1, part a), leading directly to the cyclopropane product is classified as "symmetry forbidden", because it implies a crossing of occupied and virtual orbitals.² Earlier semiempirical³ and *ab initio*⁴ studies described the addition reaction as

Chart 1



a single-step/two-phase process. In a first phase the approaching molecules are oriented in such a way as to allow an electrophilic interaction of the carbene π -system with the ethene π -system (this “ π -approach”, endowed with C_s symmetry, is sketched in Chart 1, part b). This first phase is then followed by a rotation and sideways shift of the CX₂ group, as shown in Chart 1, part c. The second part of the reaction path can be seen as a nucleophilic phase (“ σ approach”), leading to the formation of a new carbon–carbon σ -bond, while C_{2v} symmetry is approached only in the last part of the reaction path, which leads to the final product (Chart 1, part d).

The transition structure for the cycloaddition process can be located either in the electrophilic or in the nucleophilic part of the reaction path, depending on the nature of the attacking carbene.^{5,6} In the case of electrophilic and more reactive carbenes, such as CCl₂ and CF₂ (which are expected to have rather early transition states and low activation energies), the transition structure should still reflect the electrophilic nature of the π -approach; in contrast, less reactive and nucleophilic carbenes, such as C(OH)₂ (for which a later transition state and higher activation energy are expected) should exhibit more pronounced σ -bonding between the two moieties in the transition structure and a geometry closer to that of the product. This point has been illustrated by Houk and co-workers,⁶ who first examined the addi-

tion to ethene of a series of carbenes of increasing selectivity by performing RHF structure optimizations followed by MP2 single-point energy computations.

The main purpose of this paper is to discuss the existence of singlet diradical intermediates⁷ in the attack of singlet carbenes to the ethene double bond. A second related purpose is to assess if loss of stereospecificity, usually assumed as a likely outcome if triplet carbenes are involved,^{1a} might occur also in some cases of singlet carbene attack. Nonstereospecific singlet cheletropic cycloadditions have been reported⁸ in which a complex of the PhHgCBr₃ reagent with a CBr₂CHRCXY diradical was indeed postulated (R = Ph, CN; X = H, D; Y = CN, H). Isomerization could then potentially take place through a rotation of the terminal CRR' group of a singlet diradical intermediate, if it exists and if its lifetime is long enough.

Method

The study of the title reactions was performed by determining, on the reaction energy hypersurfaces, the critical points corresponding to stable structures and transition structures. The relevant geometrical parameters have been fully optimized using gradient optimization procedures⁹ at the CAS-MCSCF level of theory.¹⁰ The active space consists of the π , π^* couple of ethene and the σ -HOMO, π -LUMO of the carbenic moiety: it thus includes the orbitals of the separated reactants which are more directly involved in bond making and breaking. The computations have been carried out using the GAUSSIAN92 system of programs¹¹ and the split-valence shell 4-31G^{12a} and 6-31G(d)^{12b} basis sets. Minima and saddle points have been characterized by diagonalization of the CAS-MCSCF/4-31G analytically calculated Hessian matrix (vibrational frequencies calculation). Dynamic correlation effects have been introduced through perturbative multireference MP2 computations¹³ (MR-MP2 in the following sections), in conjunction with the 6-31G(d) basis set and using the CAS-MCSCF/6-31G(d)-optimized geometries. In the figures of the following section these optimum parameters are reported: interatomic distances are in angstroms and angles in degrees (dihedral angles are reported in parentheses).

Results and Discussion

Singlet Hypersurface. Through the use of the MC-SCF level of theory, both closed-shell species and transition or intermediate structures endowed with some

(2) Woodward, R. B.; Hoffmann, R. *The Conservation of Orbital Symmetry*; Verlag Chemie and Academic Press: Weinheim and New York, 1970. Longuet-Higgins, H. C.; Abrahamson, E. W. *J. Am. Chem. Soc.* **1965**, *87*, 2045–2046. Hoffmann, R.; Woodward, R. B. *J. Am. Chem. Soc.* **1965**, *87*, 2046–2048. Hoffmann, R. *Trans. N. Y. Acad. Sci.*, *II* **1968**, *28*, 475. Hoffmann, R.; Woodward, R. B. *Acc. Chem. Res.* **1968**, *1*, 17–22. Salem, L.; Leforestier, C.; Segal, G.; Wetmore, R. *J. Am. Chem. Soc.* **1975**, *97*, 479–487.

(3) Hoffmann, R. *J. Am. Chem. Soc.* **1968**, *90*, 1475–1485. Bodor, N.; Dewar, M. J. S.; Wasson, J. S. *J. Am. Chem. Soc.* **1972**, *94*, 9095–9102. Hoffmann, R.; Hayes, D. M.; Skell, P. S. *J. Phys. Chem.* **1972**, *76*, 664–669. Kollmar, H. J. *J. Am. Chem. Soc.* **1978**, *100*, 2660–2664.

(4) Zurawski, B.; Kutzelnigg, W. *J. Am. Chem. Soc.* **1978**, *100*, 2654–2659.

(5) (a) Moss, R. A. *Acc. Chem. Res.* **1980**, *13*, 58–64. However, reactivity and selectivity patterns depend not only on the enthalpy term but also on entropy differences; a temperature dependence of both properties has been detected several times in the past. See, for instance: (b) Skell, P. S.; Cholod, M. S. *J. Am. Chem. Soc.* **1969**, *91*, 7131–7137. (c) Giese, B.; Meister, J. *Angew. Chem., Int. Ed. Engl.* **1978**, *17*, 595–596. (d) Giese, B.; Neumann, C. *Tetrahedron Lett.* **1982**, *23*, 3557–3560. (e) Giese, B.; Lee, W.-B. *Tetrahedron Lett.* **1982**, *23*, 3561–3564. See also ref 6c.

(6) (a) Rondan, N. G.; Houk, K. N.; Moss, R. A. *J. Am. Chem. Soc.* **1980**, *102*, 1770–1776. (b) Houk, K. N.; Rondan, N. G.; Mareda, J. J. *J. Am. Chem. Soc.* **1984**, *106*, 4291–4293. (c) Houk, K. N.; Rondan, N. G. *J. Am. Chem. Soc.* **1984**, *106*, 4293–4294.

(7) Diradicals have been recently studied theoretically as intermediates in the stereomutation processes involving cyclopropanes: Getty, S. J.; Davidson, E. R.; Borden, W. T. *J. Am. Chem. Soc.* **1992**, *114*, 2085–2093. Getty, S. J.; Hrovat, D. A.; Borden, W. T. *J. Am. Chem. Soc.* **1994**, *116*, 1521–1527.

(8) Lambert, J. B.; Larson, E. G.; Bosch, R. J. *Tetrahedron Lett.* **1983**, *24*, 3799–3802. The intervention of the zwitterionic intermediate R₂C⁺–CR₂–C[–]Br₂ had been suggested in Skell, P. S.; Garner, A. Y. *J. Am. Chem. Soc.* **1956**, *78*, 5430–5433.

(9) Schlegel, H. B. In *Computational Theoretical Organic Chemistry*; Csizmadia, I. G.; Daudel, R., Eds.; D. Reidel Publishing Co.: Dordrecht, 1981; p 129. Schlegel, H. B. *J. Chem. Phys.* **1982**, *77*, 3676–3681. Schlegel, H. B.; Binkley, J. S.; Pople, J. A. *J. Chem. Phys.* **1984**, *80*, 1976–1981. Schlegel, H. B. *J. Comput. Chem.* **1982**, *3*, 214–218.

(10) Hegarty, D.; Robb, M. A. *Mol. Phys.* **1979**, *38*, 1795–1812.

(11) Frisch, M. J.; Trucks, G. W.; Head-Gordon, M.; Gill, P. M. W.; Wong, M. W.; Foresman, J. B.; Johnson, B. G.; Schlegel, H. B.; Robb, M. A.; Replogle, E. S.; Gomperts, R.; Andres, J. L.; Ragavachari, K.; Binkley, J. S.; Gonzales, C.; Martin, R. I.; Fox, D. J.; Defrees, D. J.; Baker, J.; Stewart, J. J. P.; Pople, J. A. Gaussian Inc., Pittsburgh, PA, 1992.

(12) (a) Ditchfield, R.; Hehre, W. J.; Pople, J. A. *J. Chem. Phys.* **1971**, *54*, 724–728. (b) Hariharan, P. C.; Pople, J. A. *Theoret. Chim. Acta* **1973**, *28*, 213–222.

(13) (a) Møller, C.; Plesset, M. S. *Phys. Rev.* **1934**, *46*, 618. (b) McDouall, J. J.; Peasley, K.; Robb, M. A. *Chem. Phys. Lett.* **1988**, *148*, 183–189.

Table 1. Total^a and Relative^b Energies of the Critical Points on the Singlet Surface

no.	MCSCF/4-31G			MCSCF/6-31G(d)			MR-MP2/6-31G(d)			
	<i>E</i>	ΔE^c	ΔE^d	<i>E</i>	ΔE^c	ΔE^d	<i>E</i>	ΔE^c	ΔE^d	
C(OH) ₂										
dissoen limit	-266.341 539	0.0		-266.768 210	0.0		-267.437 779	0.0		
<i>C</i> _{2v} saddle point	1a	-266.263 675	68.2							
dirad dissoci TS	2a	-266.333 269	24.5	14.7	-266.721 846	29.1	10.5	-267.405 112	20.5	12.7
dirad min	3a	-266.356 739	15.1	0.0	-266.738 657	18.5	0.0	-267.425 312	7.8	0.0
ring closure TS	4a	-266.356 140		0.4	-266.738 469	18.7	0.1	-267.427 726	6.3	-1.5
CH ₂ rotation TS	5a	-266.346 193		6.6	-266.720 331	30.0	11.5	-267.406 075	19.9	8.4
CF ₂										
dissoen limit	-314.281 653	0.0		-314.741 083	0.0		-315.392 426	0.0		
<i>C</i> _{2v} saddle point	1b	-314.225 514	54.4							
dirad dissoci TS	2b	-314.295 040	10.8	16.0	-314.712 087	18.2	13.5	-315.374 678	11.1	15.6
dirad min	3b	-314.320 507	-5.2	0.0	-314.733 566	4.7	0.0	-315.399 599	-4.5	0.0
ring closure TS	4b	-314.315 747		3.0	-314.729 323	7.4	2.7	-315.402 824	-6.5	-2.0
CH ₂ rotation TS	5b	-314.309 916		6.6	-314.721 676	12.2	7.5	-315.387 559	3.0	7.5

^a hartree. ^b kcal mol⁻¹. ^c With respect to the dissociation limit. ^d With respect to the diradical intermediate.

diradicaloid nature (which cannot be properly studied at the Hartree–Fock level) can be described with a similar degree of accuracy. This approach allowed us to check the reliability of the description of the reaction energy hypersurface obtained at the single determinant level of theory. Indeed, the intervention of diradical intermediates was detected, offering a qualitatively different picture of the reaction path. The following approaches of the two carbene species to ethene were investigated in the case of the singlet reaction: (a) a *C*_{2v} “symmetry forbidden” attack and (b) a *C*_s “symmetry allowed” approach (both are shown in Chart 1). Moreover, the possible existence of stable or transition *C*₁ structures, similar to those found on the triplet surface (see below), was tested, in order to assess if lower-symmetry pathways were available also on the singlet surface. In the following discussion, use will be generally made of the CAS-MCSCF/6-31G(d) energy results, unless otherwise specified; dynamic correlation effects introduced by the MR-MP2 calculations will be commented on separately at the end of the singlet and triplet subsections.

A. *C*_{2v} Forbidden Approach. The critical points found in correspondence of this mode of attack occur at a rather large distance between the two moieties in all the cases examined. The energy of these structures is significantly high, and higher for C(OH)₂ than for CF₂ (see Table 1);^{14a} this result confirms the predictions of simple qualitative theories.

Moreover, on the basis of the vibrational analysis, all these structures are classified as second-order saddle points, of no chemical interest. Due their the limited importance, these structures were studied only at the CAS-MCSCF/4-31G level (the optimized geometries are shown in Figure 1). This result rules out, as expected, the possibility of a viable *C*_{2v} pathway for this kind of cheletropic cycloaddition. The two directions of negative curvature on the energy hypersurface (corresponding to imaginary frequencies) are dominated first by the distance *R*, defined between the carbenic carbon and the carbon–carbon bond in ethene (Chart 1, part a) and second by the opening of the α angle, defined by the carbenic carbon, the midpoint X on the ethene CC bond, and one ethene carbon (Chart 1, part a), which would

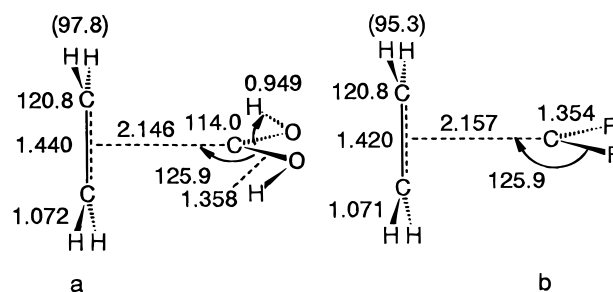


Figure 1. Singlet reaction. The second-order saddle points corresponding to the *C*_{2v} forbidden approach.

cause the breaking of the *C*_{2v} symmetry. If the *C*_{2v} symmetry constraint is relaxed following this second direction, structures pertaining to a pathway possibly endowed with *C*_s symmetry are to be looked for.

Diradicaloid Pathway. For each of the two carbenes, four critical points were found along this pathway. As the two reactants approach from infinite separation, first a loosely bound π -complex is found, whose structure is close to that depicted in Chart 1, part b.¹⁵ These shallow minima are located at an intermolecular distance of ca. 3.4–3.8 Å (for CF₂ and C(OH)₂, respectively); the other geometrical parameters do not depart significantly from those optimized for the separate reactants. In both cases their energy is just about 1 kcal mol⁻¹ below the that of the separated reagents. These depressions on the energy surfaces could as well be mere computational artifacts, due to a basis set superposition error. Due to the limited interest of these complexes, they were not investigated any further. In ref 6b Houk et al. have already discussed the possible existence of loosely bound π -complexes in halocarbene cheletropic reactions, concluding that species of this kind are not likely to be present on free-energy hypersurfaces.

Three other critical points were found for both C₂H₄ + C(OH)₂ and C₂H₄ + CF₂ reactions on this pathway. As the two reactants get closer, the dominium of a first-order saddle point is entered.^{14b} The optimum *C*_s geometries shown in Figure 2 indicate that the relevant transition structures are related to the *C*_{2v} second order saddle points by the α angle opening mentioned above (Chart 1, part a). The transition vector is dominated by the intermolecular distance *D*, defined in Chart 1, part c, as

(14) (a) The surface for methylene addition to ethene has already been studied by other researchers (see for instance refs 4, 6, and 7). At the MCSCF/4-31G level the *C*_{2v} barrier (relevant to a second-order saddle point) is computed to be lower than those reported in Table 1 (26.0 kcal mol⁻¹). (b) In a parallel way, no barrier is found in correspondence of a *C*_s attack.

(15) The intervention of π -complexes has been suggested on the basis of experimental results: Giese, B.; Lee, W.-B.; Neumann, C. *Angew. Chem., Int. Ed. Engl.* **1982**, *21*, 310.

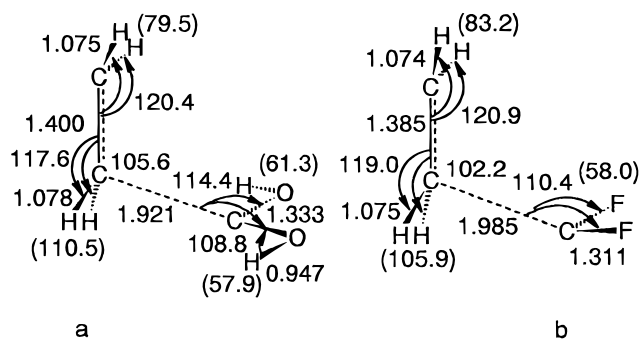


Figure 2. Singlet reaction. The transition structures for diradical formation (or dissociation).

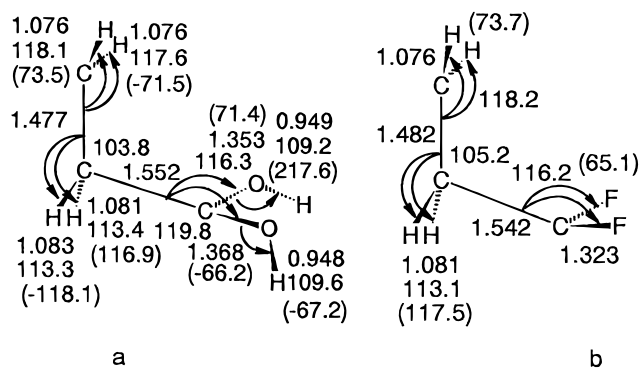


Figure 3. Singlet reaction. The diradical intermediates.

that between the carbenic carbon and the closer carbon atom in ethene (with a coefficient of 0.92 in both cases). Although both transition structures occur at a *D* distance of ca. 2 Å, the CF₂ transition structure appears to be slightly earlier, in a geometrical sense, having longer *D* and shorter ethene C–C distances (Figure 2). Consistent with these data, the energy barrier with respect to the separate reactants is higher by ca. 10 kcal mol⁻¹ for C(OH)₂. Therefore, the present calculations describe difluorocarbene as more reactive and electrophilic than dihydroxycarbene.

Up to this point the results obtained for the allowed approach seem to be in qualitative agreement with previous results, obtained at the RHF level of theory.⁶ However, the transition structures **2a** and **2b** do not lead directly to the addition products, as would be the case for a very asynchronous but still one-step reaction: instead, two CX₂CH₂CH₂ intermediates of diradical character are present for both reactions on the energy hypersurfaces as well-defined minima,⁷ and consequently these reactions are described, at the CAS-MCSCF level of theory, as nonconcerted. The structures of the diradical intermediates are shown in Figure 3, in which it can be seen that only **3b** has retained the *C_s* symmetry of the preceding transition structure, while **3a** is *C₁*. Their stability with respect to the dissociation limit is significantly different: the F disubstituted diradical **3b** is more stable than the OH disubstituted **3a** by ca. 12 kcal mol⁻¹ (Table 1). Nevertheless, both are stable with respect to redissociation to the separated reactants: the barriers for the backward process, which would take place through the diradicaloid transition structures **2a** and **2b**, are higher than 10 kcal mol⁻¹ in both cases (Table 1).

Ring closure to the products takes place through a second kinetic step. The two transition structures for the cyclopropanation step are shown in Figure 4, and the corresponding energy barriers, reported in Table 1, are

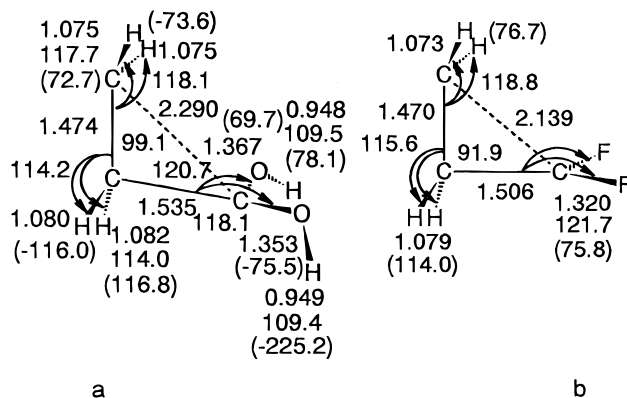


Figure 4. Singlet reaction. Ring closure transition structures.

found to be low: therefore, the rate-determining step is the formation of the two diradical intermediates. In the case of the C(OH)₂ diradical, the MCSCF barrier is significantly lower than that in the CF₂ case to such an extent to suggest some doubts on the real importance of the presence of the diradical intermediate. The two transition structures differ in a consistent way: **4a** appears to be earlier, in a geometrical sense, than **4b**, as can be observed by comparing again, for instance, the CCC angles (indicated as β in Chart 1, part c), which have undergone a change of -4.7° and -13.3° in the OH and F cases, respectively, or, equivalently, the two carbon-carbon distances indicated as dashed lines in Figure 4. The transition structure **4a** is also slightly asymmetric (*C₁*), while **4b** is *C_s*.

B. The Isomerization Process. The loss of stereospecificity is usually assumed to be a likely outcome if triplet carbenes are involved.^{1a} Nevertheless, the description of the potential energy hypersurfaces just discussed opens this possibility for the singlet-carbene cyclopropanation reactions too, at least in the case of the difluoro system, which presents a higher barrier for ring closure. As mentioned in the Introduction, nonstereospecific singlet cheletropic cycloadditions have been reported.⁸ In the case of lack of stereospecificity, isomerization could then take place through rotation (or rotation plus inversion) of the terminal CRR' group in the diradical intermediate (Scheme 2), provided that its lifetime can be long enough.

In the present study, dealing with simple models, the barrier for rotation of the terminal methylenic group in the CX₂CH₂CH₂ diradicals was determined, in order to compare its height with that relevant to ring closure. Considering that the systems studied here lack any extra stabilization (as the one suggested in ref 8, operated on the diradical intermediate by the Seyferth reagent), the purpose of this investigation can just be that of assessing if the rotational barrier is of the same order of magnitude of the barrier to ring closure. The transition structures relevant to the isomerization pathway are shown in Figure 5. These are sheer rotational transition structures and appear to be the only transition structures present on the topomerization surface. They can be thought of as connecting the diradical minima **a** to their isomers **a'** (in the present case **a** and **a'** are identical structures; see Scheme 2). Indeed, attempts to find rotation-inversion transition structures, as **b**, located only second order saddle points, while gauche structures as **d** are not present as minima, evolving to **a'** without any energy barrier. Therefore, the isomerization pathway goes only through a rotational transition structure

Table 2. Singlet Surface: Ring Closure and Isomerization Activation Free Energies^a

	218 K			298 K			378 K		
	ΔH^\ddagger	$-T\Delta S^\ddagger$	ΔG^\ddagger	ΔH^\ddagger	$-T\Delta S^\ddagger$	ΔG^\ddagger	ΔH^\ddagger	$-T\Delta S^\ddagger$	ΔG^\ddagger
C(OH) ₂									
ring closure	-0.2	0.2	<0.1	-0.3	0.4	0.1	0.4 ₅	0.7	0.3
CH ₂ rotation	5.7	-0.1	5.6	5.6	<0.1	5.6	5.5	0.1	5.6
CF ₂									
ring closure	2.5	0.3	2.8	2.4	0.5	2.9	2.3	0.8	3.0
CH ₂ rotation	5.5	-0.4	5.1	5.5	-0.6	4.9	5.4	-0.6	4.8

^a kcal mol⁻¹; all quantities computed at the MCSCF/4-31G level, with respect to the diradical intermediates.

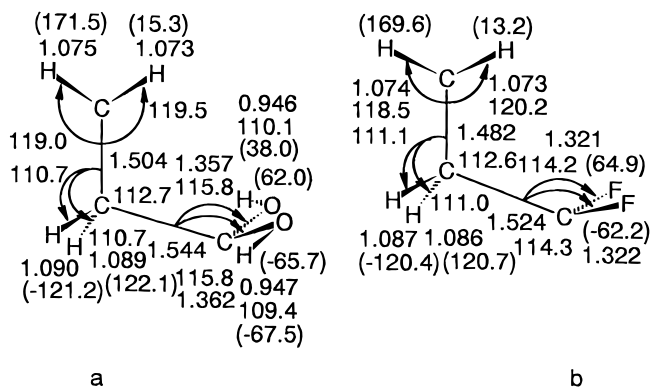
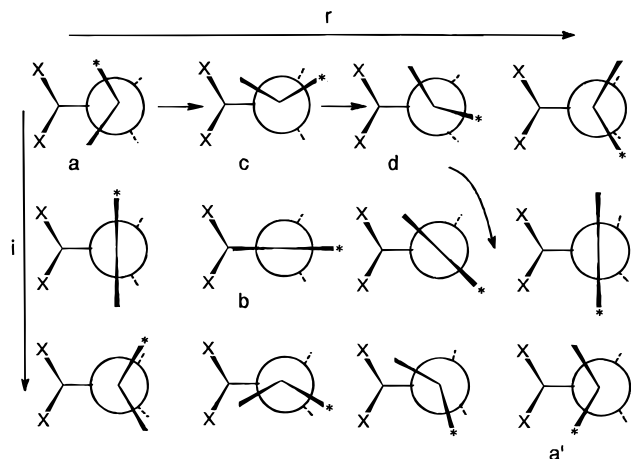


Figure 5. Singlet reaction. The rotational transition structures relevant to the isomerization pathway.

Scheme 2

of the CX₂CH₂CH₂ diradical, **c**, approximately following the arrows in Scheme 2 (this exploration was carried out at the 4-31G level only). The relevant energy barriers are in both cases higher than the barriers for ring closure, although less so in the case of the difluoro intermediate. From Table 1 it can be seen that the ΔE^\ddagger values are more different in the case X = OH.

The role of the enthalpic and entropic contributions to the activation free energy of the two processes has also been studied. Isomerization and ring closure ΔG^\ddagger values were computed at the MCSCF/4-31G level only, at which the vibrational analysis had been carried out. These values, determined for three different temperatures, are reported in Table 2. In the case of the fluorinated diradical, the ring closure ΔH^\ddagger term is lower than the ΔE^\ddagger reported in Table 1 by 0.5 kcal mol⁻¹, while for methylene rotation it is lower by 1.1 kcal mol⁻¹. Similarly, the $-T\Delta S^\ddagger$ term operates in favor of the methylene rotation process and against ring closure, although it provides a smaller contribution. Obviously, the higher the temperature, the stronger the effect: thus, in the case

of the CH₂CH₂CF₂ diradical, at a not unreasonable temperature of ca. 80 °C, the two pathways are described as becoming more competitive. In the case of the CH₂-CH₂C(OH)₂ diradical, on the other hand, the initial difference between activation energies is too large for allowing a reversal of the preferences. Although the approximations used in evaluating these thermodynamic quantities (ideal gas, harmonic oscillator, rigid rotor) suggest the use of some prudence in drawing conclusions, it appears not unreasonable to consider the possibility of a partial isomerization process in some singlet-carbene cycloadditions, if carried out at rather high temperatures (besides, structural factors could in some specific cases further stabilize the isomerization pathway, as proposed in ref 8).

Comparing the MR-MP2//MCSCF and MCSCF energy profiles (Table 1), it can be noted that, as a general effect, the inclusion of dynamic correlation (through the MR-MP2 approach) has the effect of lowering the energy barriers for the first step (diradical formation). This step is also described as less endothermic, or even exothermic in the case of fluorine. Within the obvious limitations of the information provided by single-point energy computations, the topology itself of the potential energy surface would appear to be affected by dynamic correlation: indeed, for the singlet state the shallow minima corresponding to diradical intermediates seem to disappear altogether.¹⁶

Triplet Hypersurface. The addition of the same two carbenes in their triplet state¹⁷ to ethene was studied in a similar way. The triplet states of CF₂ and C(OH)₂ are estimated to lie above the corresponding singlet, by 47.5 and 51.5 kcal mol⁻¹, respectively, at the CAS-MCSCF level (by 46.1 and 49.8 kcal mol⁻¹ at the MR-MP2 level). The first figure can be compared with the recent estimate of 56.4 kcal mol⁻¹ obtained by Irikura, Goddard, and Beauchamp.¹⁸ Both reactions are described as proceeding through transition and stable structures endowed with diradical character. The two transition structures which lead to formation of the diradical intermediates are shown in Figure 6. It can be seen that their geometries are less symmetric than those found on the singlet hypersurface. In both cases, for diradical formation, the triplet reactions require the overcoming of

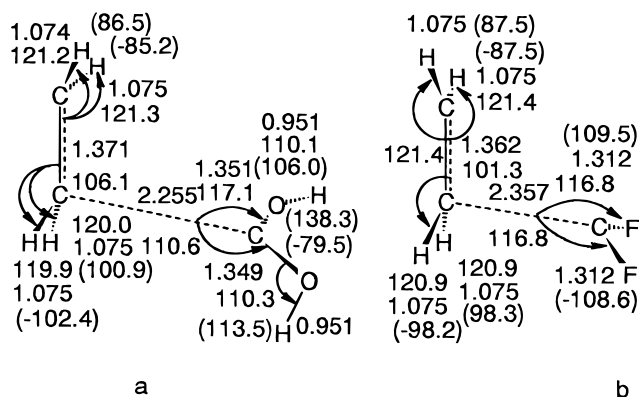
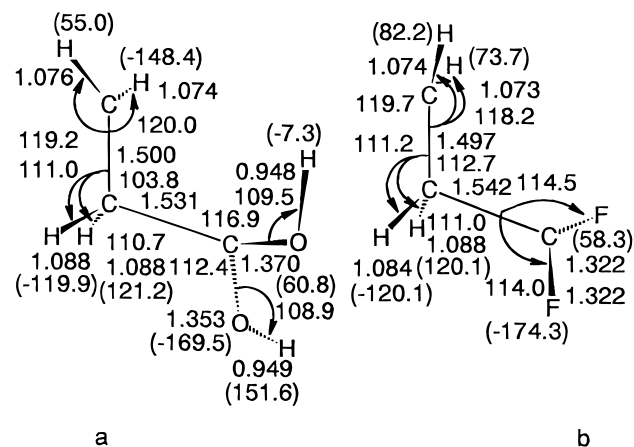
(16) However, it can be considered that the common procedure of carrying out single-point energy calculations actually probes in an arbitrary way the higher-level energy hypersurface. Therefore, it seems to be reasonable to contemplate the possibility that the transition structure on the MR-MP2 surface might simply be earlier in a geometrical sense: in this case, the probing performed by using the geometries determined at a lower theoretical level would occur in a zone of descent on the higher-level surface, i.e., beyond the MR-MP2 first-order saddle point.

(17) For a UHF and MP2 study on the reactivity of triplet carbenes, compare: Moreno, M.; LLuch, J. M.; Oliva, A.; Bertràn, J. *J. Mol. Struct. (Theochem)* **1988**, *164*, 17–24.

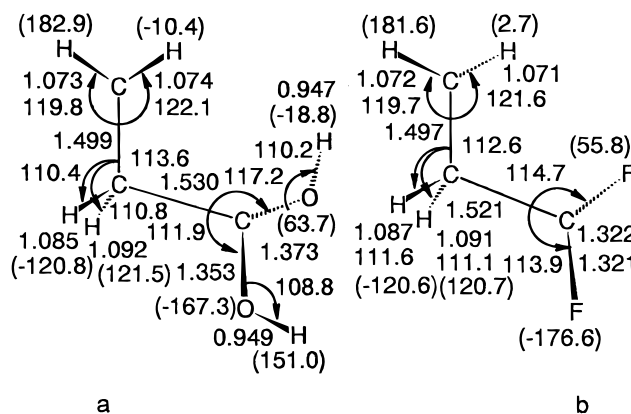
(18) Irikura, K. K.; Goddard, W. A., III; Beauchamp, J. L. *J. Am. Chem. Soc.* **1992**, *114*, 48–51.

Table 3. Total^a and Relative^b Energies of the Critical Points on the Triplet Surface

	MCSCF/4-31G		MCSCF/6-31G(d)		MR-MP2/6-31G(d)	
	<i>E</i>	ΔE^c	<i>E</i>	ΔE^c	<i>E</i>	ΔE^c
C(OH) ₂						
disson limit	-266.309 113	0.0	-266.686 092	0.0	-267.358 435	0.0
dirad dissociation TS	6a	-266.297 382	-266.672 013	8.8	-267.349 533	5.6
diradical min	7a	-266.350 164	-266.730 321	-27.8	-267.416 826	-36.6
CH ₂ rotation TS	8a	-266.349 135	-266.727 613	-26.1	-267.414 673	-35.3
CF ₂						
disson limit	-314.258 889	0.0	-314.665 458	0.0	-315.318 893	0.0
dirad dissociation TS	6b	-314.253 817	-314.657 729	4.8	-315.315 674	2.0
diradical min	7b	-314.313 324	-314.724 653	-37.1	-315.389 503	-44.3
CH ₂ rotation TS	8b	-314.312 019	-314.723 252	-36.3	-315.389 857	-44.5

^a hartree. ^b kcal mol⁻¹.**Figure 6.** Triplet reaction. The two transition structures leading to the formation of diradical intermediates.**Figure 7.** Triplet reaction. The diradical intermediates.

energy barriers (Table 2) lower than those encountered on the singlet surface. The CX₂CH₂CH₂ diradical intermediates are shown in Figure 7. Their stability with respect to back-dissociation to the original reactant moieties is also more than three times higher than that in the singlet case: 42–46 kcal mol⁻¹ are required in the case X = F, 37–42 kcal mol⁻¹ in the case X = OH. The model isomerization processes in these simple systems could again take place through rotation of the terminal methylenic group: the relevant rotational transition structures are reported in Figure 8. The two energy barriers for CH₂ rotation are significantly lower than those computed for the analogous singlet diradicals (Table 3). The reason could be traced back to the loss, on rotation, of a favorable spin interaction between the opposing terminal carbons, which is present in the singlet and not in the triplet.

**Figure 8.** Triplet reaction. The rotational transition structures relevant to the isomerization pathway.

Comparing the MR-MP2/MCSCF and MCSCF energy profiles (Table 3), it can be noted that the inclusion of dynamic correlation has the effect of lowering the energy barrier for diradical formation and that for methylene rotation. The formation of the diradical is also described as more exothermic. For the triplet state the topology of the potential energy surface does not appear to be affected by dynamic correlation.

Interpretation of the Trends Observed on the Singlet and Triplet Hypersurfaces. A simple diabatic model based upon spin recoupling in VB theory¹⁹ can be used to understand the nature of the transition state for diradical formation (which is completely different from that of the transition state for ring closure) and the increase of energy barrier on passing from CF₂ to C(OH)₂. In this model the total energy profile is decomposed into two component curves: one, associated with the reactant spin coupling (reactant bonding situation), is indicated as *reactant diabatic* and the other, associated with the product spin coupling (product bonding situation), is denoted as *product diabatic*. In this model, the transition state for singlet diradical formation originates from the avoided crossing between the reactant diabatic curve, which is destabilized as the reaction proceeds, and the product diabatic, which is stabilized.

The qualitative behavior of the two diabatals for the addition of CF₂ and C(OH)₂ to ethene is represented in Figure 9. For sake of comparison the case of methylene (CH₂) is also considered, for the hypothetical reaction leading to the trimethylene diradical. The reactant diabatic corresponds to singlet ethene + singlet carbene

(19) Pross, A.; Shaik, S. S. *Acc. Chem. Res.* **1983**, *16*, 363. Bernardi, F.; Olivucci, M.; McDouall, J. J. W.; Robb, M. A. *J. Chem. Phys.* **1988**, *89*, 6365.

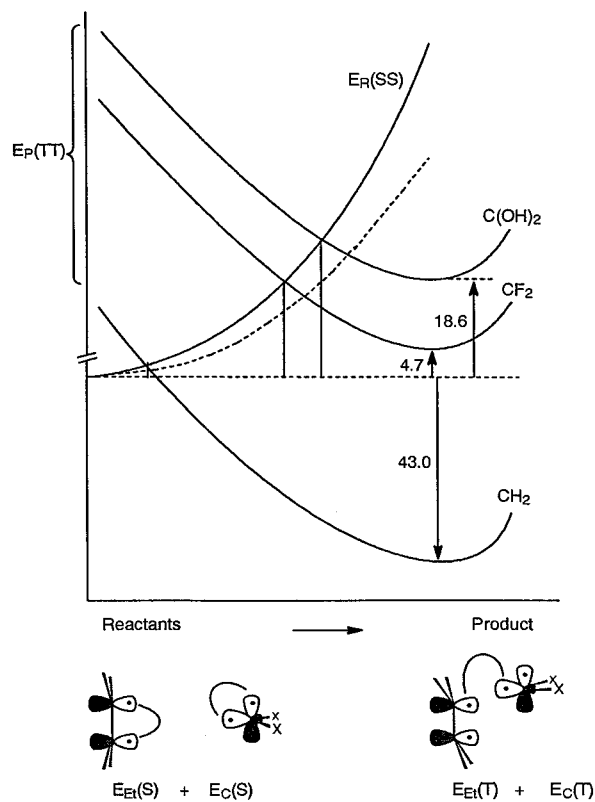


Figure 9. Diabatic curve crossings leading to energy barriers of different height for diradical formation. Solid lines correspond to a geometry of attack with a smaller β angle (Chart 1, part c), while a dashed line corresponds to a larger β angle. See text for details.

(reactant coupling SS), while the product diabatic involves triplet ethene + triplet carbene coupled to an overall singlet state (product coupling TT). The diagrams reported in Figure 9 are based on the following assumptions. (i) The product diabatals at the product geometry are positioned with respect to the reactant diabatals at the reactant geometry on the basis of the computed total energies. (ii) A common reference energy level for reactants has been assumed in all three cases. (iii) The energy difference between the two diabatals is given by:

$$E_P(\text{TT}) - E_R(\text{SS}) = [E_{\text{Et}}(\text{T}) + E_{\text{C}}(\text{T})] - [E_{\text{Et}}(\text{S}) + E_{\text{C}}(\text{S})] = [E_{\text{Et}}(\text{T}) - E_{\text{Et}}(\text{S})] + [E_{\text{C}}(\text{T}) - E_{\text{C}}(\text{S})] = \Delta E_{\text{Et}} + \Delta E_{\text{C}}$$

where $E_P(\text{TT})$ and $E_R(\text{SS})$ are the energies of the product and reactant diabatals, respectively; E_{Et} denotes the energy values of triplet (T) and singlet (S) ethene; and E_{C} denotes the energy values of triplet and singlet carbenes. Since the quantity ΔE_{Et} is the same in the various reactions, the key factor that controls the relative magnitude of the energy barrier in the various cases is ΔE_{C} . This quantity is negative for CH_2 ($-12 \text{ kcal mol}^{-1}$ at the MCSCF level) where the triplet is the ground state. The computations show that ΔE_{C} is smaller for CF_2 than for $\text{C}(\text{OH})_2$ (47.5 and 51.5 kcal mol^{-1} at the MCSCF level, respectively). (iv) The slope of the reactant diabatals can be assumed to be approximately the same in the three cases since it depends mainly on the repulsion between the doubly occupied orbital of singlet carbene and the π -orbital of ethene.

Inspection of the diagram reported in Figure 9 shows the following features. (i) The barrier for diradical

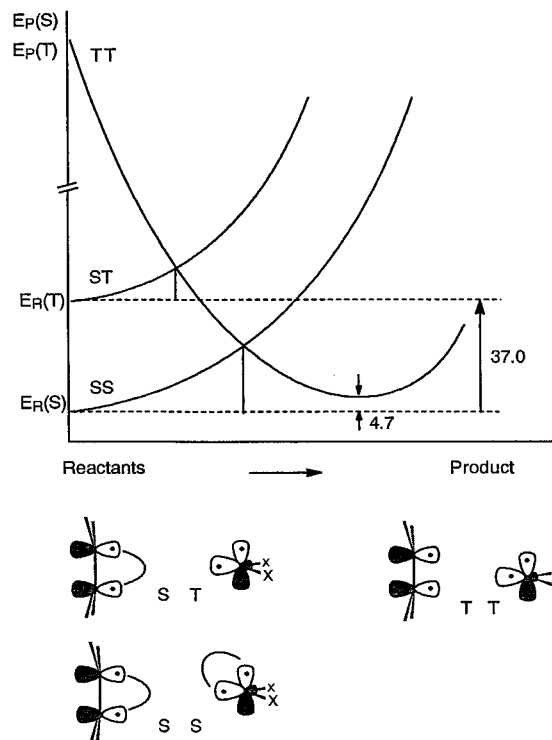


Figure 10. Diabatic curve crossings leading to energy barriers of different height for singlet and triplet diradical formation (ethene + difluorocarbene reaction). See text for details.

formation is the largest in correspondence of the attack of $\text{C}(\text{OH})_2$, followed by that associated with the attack of CF_2 , i.e., $\Delta E(\text{C}(\text{OH})_2) > \Delta E(\text{CF}_2) > \Delta E(\text{CH}_2)$, as shown by the values listed in Table 1. (ii) The reactant diabatic is less repulsive with the increase of the CCC β angle (see Chart 1, part c). This corresponds to a change from the ascending full line to the analogous dashed line, both representing reactant diabatic curves for each type of attack. Thus the barriers tend to decrease with the increase of the β angle, in agreement with the values associated with C_{2v} and C_s geometries (Table 1). (iii) The intercarbon D distances (Chart 1, part c) follow the order $D(\text{C}(\text{OH})_2) < D(\text{CF}_2) < D(\text{CH}_2)$, as shown by the results of Figure 2. Therefore Figure 9 summarizes the main energetic and geometrical features found for the transition states for diradical formation. On the other hand, the nature of the transition states for ring closure is not associated to any avoided crossing, since this type of transition state is found in a region of the potential energy surface dominated only by the product diabatic. Thus, while the transition states for diradical formation are sensitive to electronic effects, those for ring closure are sensitive to geometric effects.

This type of diabatic analysis rationalizes also the different features of singlet and triplet diradical transition structures and intermediates. The relevant diabatic curves are compared in Figure 10, where on the reactant side are reported, in order of increasing energy, the following spin coupling situations (the energy difference values refer to the MCSCF/6-31G(d) results for $\text{H}_2\text{C}=\text{CH}_2 + \text{CF}_2$): (i) the singlet reactant situation, where singlet ethene + singlet carbene (SS) are coupled to an overall singlet state (the related energy is denoted as $E_R(\text{S})$); (ii) the triplet reactant situation, where singlet ethene + triplet carbene (ST) are coupled to an overall triplet state (the related energy is denoted as $E_R(\text{T})$); (iii) the singlet and triplet product situation, where triplet ethene +

triplet carbene (TT) are coupled to an overall singlet or triplet state (the related energies are denoted as $E_p(S)$, $E_p(T)$). Along the reaction coordinate, which corresponds mainly to C–C bond formation in the diradicals, both reactant situations are repulsive, while both product situations are attractive and almost degenerate (hence, a single curve is reported for simplicity in Figure 10). The analysis of the resulting diabatic curves shows the following features: (i) the crossing for the triplet process occurs earlier than that for the singlet process, in agreement with the computed C–C bond distances in the diradical transition structures (see Figures 2 and 6), which are larger in the triplet transition structures; (ii) the activation barrier, related to the energy difference between the crossing and the reactants, is larger for the singlet than for the triplet, in agreement with the data listed in Tables 1 and 3; (iii) the fragmentation barrier, i.e., the energy difference between the diradical and the crossing is smaller for the singlet process (later crossing) than for the triplet (earlier crossing).

Reaction with Bulky Substituted Alkenes. As shown by the diabatic analysis, the nature of the transition states for ring closure is not associated to any avoided crossing, since this type of saddle point is found in a region of the potential energy surface dominated only by the product diabatic. Thus, while the transition states for diradical formation are more sensitive to electronic effects, those for ring closure are expected to exhibit some dependence from geometric effects. For this reason, the attack of singlet CF₂ to isobutene was also investigated, in order to assess if bulky substituents on the double bond can play a certain role in determining the existence of a diradical intermediate (Figure 11). At the CAS-MCSCF/6-31G(d) level, a diradical minimum was found, with a barrier to ring closure of 5.7 kcal mol⁻¹. The corresponding MR-MP2//CAS-MCSCF energy difference value (1.1 kcal mol⁻¹) suggests that even at this computational level a barrier to ring closure exists, even if significantly reduced with respect to the previous value. The stabilizing effect of the bulky substituents upon the diradical is due to two factors: (i) the radical center changes from primary (in **3b**) to the more stable tertiary (in **11a**); (ii) the repulsion between the relatively bulky methyl groups and the approaching CX₂ group (repulsion is larger in **11b** than in **4b**).

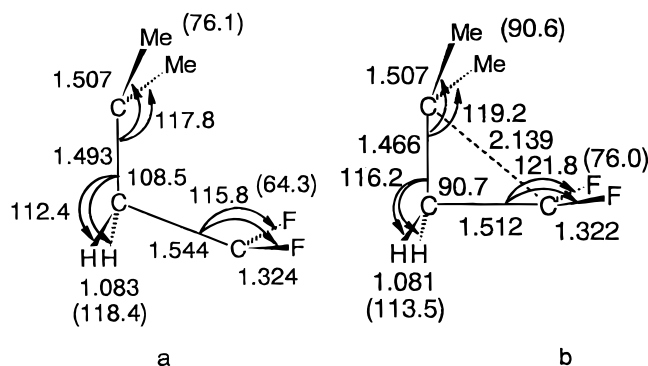


Figure 11. Reaction of singlet difluorocarbene and isobutene. (a) Diradical intermediate. (b) Ring closure transition structure.

Conclusions

We have reported in this paper the results obtained in a CAS-MCSCF and MR-MP2/6-31G(d) computational study of the reaction between singlet and triplet CF₂ and C(OH)₂ with ethene. The main conclusions (based on the MR-MP2 results) can be summarized as follows. (i) The reaction of singlet carbenes with ethene seems to proceed via a very asynchronous but concerted pathway, while the reaction of singlet CF₂ with isobutene involves the formation of a diradical intermediate. These results can be generalized by saying that, while the attack to ethene itself could be concerted, with bulky substituted alkenes the reaction can be a two-step process, with formation of a diradical intermediate. (ii) The energy barriers for methylene rotation in the triplet diradicals are significantly lower than those obtained for the analogous singlet diradicals, suggesting that loss of stereospecificity can more easily take place in triplet rather than in singlet diradicals.

Acknowledgment. Financial support from the Italian MURST and from the Italian CNR (within the project Progetto Strategico Tecnologie Chimiche Innovative) is gratefully acknowledged. An IBM RISC-6000/550 computer was assigned to GT by the Italian CNR under the project Calcolo Avanzato in Chimica. A computational grant from CSI-Piemonte is also acknowledged.

JO960860R